

A historical review of sediment export–import shift in the North Branch of Changjiang Estuary

Guo, Leicheng; Xie, Weiming; Xu, Fan; Wang, Xianye; Zhu, Chunyan; Meng, Yi; Zhang, Weiguo; He, Qing

DOI

[10.1002/esp.5084](https://doi.org/10.1002/esp.5084)

Publication date

2021

Document Version

Accepted author manuscript

Published in

Earth Surface Processes and Landforms

Citation (APA)

Guo, L., Xie, W., Xu, F., Wang, X., Zhu, C., Meng, Y., Zhang, W., & He, Q. (2021). A historical review of sediment export–import shift in the North Branch of Changjiang Estuary. *Earth Surface Processes and Landforms*, 47(1), 5-16. <https://doi.org/10.1002/esp.5084>

Important note

To cite this publication, please use the final published version (if applicable). Please check the document version above.

Copyright

Other than for strictly personal use, it is not permitted to download, forward or distribute the text or part of it, without the consent of the author(s) and/or copyright holder(s), unless the work is under an open content license such as Creative Commons.

Takedown policy

Please contact us and provide details if you believe this document breaches copyrights. We will remove access to the work immediately and investigate your claim.

1 A historical review of sediment export-import shift in the North Branch
2 of Changjiang Estuary

3

4 Leicheng Guo ^{a,*}, Weiming Xie ^a, Fan Xu ^a, Xianye Wang ^a,
5 Chunyan Zhu ^{a,b}, Yi Meng ^a, Weiguo Zhang ^a, Qing He ^a

6

7 ^a State Key Lab of Estuarine and Coastal Research, East China Normal
8 University, Shanghai 200241, China

9 ^b Civil Engineering and Geosciences faculty, Delft University of Technology, PO
10 Box 5048, Delft 2600 GA, the Netherlands

11

12 * Corresponding author, E-mail: lguo@sklec.ecnu.edu.cn

13

24 **Abstract**

25 Net sediment transport is predominantly seaward in fluvial-dominated
26 estuaries worldwide. However, a distributary branch in the Changjiang Estuary,
27 the North Branch, undergoes net landward sediment transport, which leads to
28 severe channel aggradation. Its controlling mechanism and the role of human
29 activities remain insufficiently understood, although such knowledge is
30 necessary for better management and restoration opportunities. In this study
31 we revisit the centennial hydro-morphodynamic evolution of the North Branch
32 based on historical maps, field data, and satellite images and provide a
33 synthesis of the regime change from ebb to flood dominance. The North
34 Branch was once a major river and ebb-dominant distributary channel. within
35 which alternative meandering channels and sand bars developed. Deposition
36 of river-borne sediment leads to infilling of the branch, while tidal flat
37 embankment reduces the bankfull width and modifies the channel
38 configuration, resulting in a profound decline in the sub-tidal flow partition rate.
39 The North Branch then becomes tide-dominant with an occurrence of tidal
40 bores and elongated sand ridges. Once tidal dominance is established,
41 extensive tidal flat reclamation enhances the funnel-shaped planform,
42 amplifying the incoming tides and initiating a positive feedback process that
43 links tidal flat loss, sediment import, and channel aggradation. Overall, the shift
44 in branch dominance is a combined result of a natural south-eastward
45 realignment of the deltaic distributary channels and extensive reclamation.
46 One management option to mitigate channel aggradation is to stop the
47 aggressive reclamation and allow tidal flats to build up, which might reduce the
48 sediment import and eventually lead to a morphodynamic equilibrium in the
49 longer term. Understanding the impact of tidal flat reclamation is informative for
50 the management of similar tidal systems under strong human interference.

51 **Key words:** Changjiang; Morphodynamics; Flood dominance; Reclamation;
52 Regime shift

53 **1. Introduction**

54 Tidal estuaries and basins can be flood- or ebb-dominant depending on
55 the basin geometry, tidal properties, the amount of inter-tidal flats, and river
56 discharge magnitude (Friedrichs and Aubrey, 1988; Ridderinkhof et al., 2004;
57 de Swart and Zimmerman, 2009). In general, short tidal basins without
58 significant tidal flats and no river discharge are more likely to be
59 flood-dominant because tidal wave deformation in shallow waters leads to
60 shorter rising tides and stronger flood currents (Friedrichs and Aubrey, 1988;
61 Lanzoni and Seminara, 2002). The presence of a significant number of
62 inter-tidal flats tends to enhance ebb currents owing to the hydraulic storage
63 effect of inter-tidal flats (Speer and Aubrey, 1985). A (seaward) Stokes' return
64 flow in long basins may also benefit ebb dominance (van der Wegen and
65 Roelvink, 2008; Guo et al., 2014). River flow enhances tidal wave deformation
66 by prolonging the falling tide and intensifying ebb currents, which reinforces
67 ebb dominance (Guo et al., 2014). Ebb or flood dominance is defined herein as
68 the seaward or landward tide-averaged sediment transport, respectively.
69 Flood-dominant estuaries import sediment from the sea, leading to basin
70 infilling and accretion of tidal flats. In contrast, ebb-dominant systems export
71 sediment to the sea, leading to basin emptying and enlarged channel volumes.
72 The nature of tidal asymmetry plays a dominant role in controlling the
73 large-scale estuarine morphology in the longer term. Thus, it is of practical
74 importance to understand the dynamic behaviour and controlling processes of
75 tidal asymmetry.

76 While tidal asymmetry and net dominance have been extensively studied
77 in single-channel environments with minimal river discharge influence
78 (Dronkers, 1986; Ridderinkhof et al., 2004), the variability of branch dominance
79 is insufficiently studied in branched estuaries where multiple bifurcated
80 branches exhibit different dynamics. The Changjiang Estuary is such a case:
81 four branches connect to the coastal ocean, of which the South Branch and its
82 seaward channels and passages are the main conduits of river-borne

83 freshwater and sediment. In contrast, the North Branch is currently a
84 tide-dominant branch with limited river influence. Accordingly, the South
85 Branch is ebb-dominant and the North Branch is flood-dominant, where
86 sediment import leads to continued net deposition and channel aggradation
87 (Dai et al., 2016). This has raised management concerns regarding the fate of
88 the North Branch if it is expected to be continuously infilled.

89 Research on the North Branch has been limited compared with that on the
90 other parts of the Changjiang Estuary. Few studies have examined the tidal
91 bores (Chen, 2003), reverse flow and salt intrusion (Wu et al., 2006; Zhang et
92 al., 2019, 2020), and sedimentation and aggradation of the North Branch (Yun,
93 2004; Dai et al., 2016; Li et al., 2020; Obodoefuna et al., 2020). The North
94 Branch was once one of the main branches discharging riverine water and
95 sediment to the sea, implying a regime of ebb dominance, but became
96 flood-dominant since the 1950s (Yun, 2004). However, it remains poorly
97 understood how the hydrodynamic regime in the North Branch has changed
98 over time and what caused the regime shift from ebb to flood dominance. Such
99 knowledge is a prerequisite for sustainable management and restoration
100 opportunities in the North Branch and can also inform management of tidal
101 basins and estuaries elsewhere that are undergoing similar human
102 interventions and changes. For instance, land reclamation across the Pearl
103 River Delta has substantially extended the shoreline towards the sea and
104 induced shrinkage of the channel volume (Liu et al., 2019). In the Western
105 Scheldt Estuary, reclamation and dredging have similarly caused channel
106 shrinkage and tidal amplification (de Vriend et al., 2011). In this study, we
107 provide a synthesis of the centennial hydro-morphodynamic evolution of the
108 North Branch based on field data to clarify historical changes and the impact of
109 human activities. Further exploration of the governing mechanisms by using a
110 numerical hydro-morphodynamic model will be presented in a future paper.

111

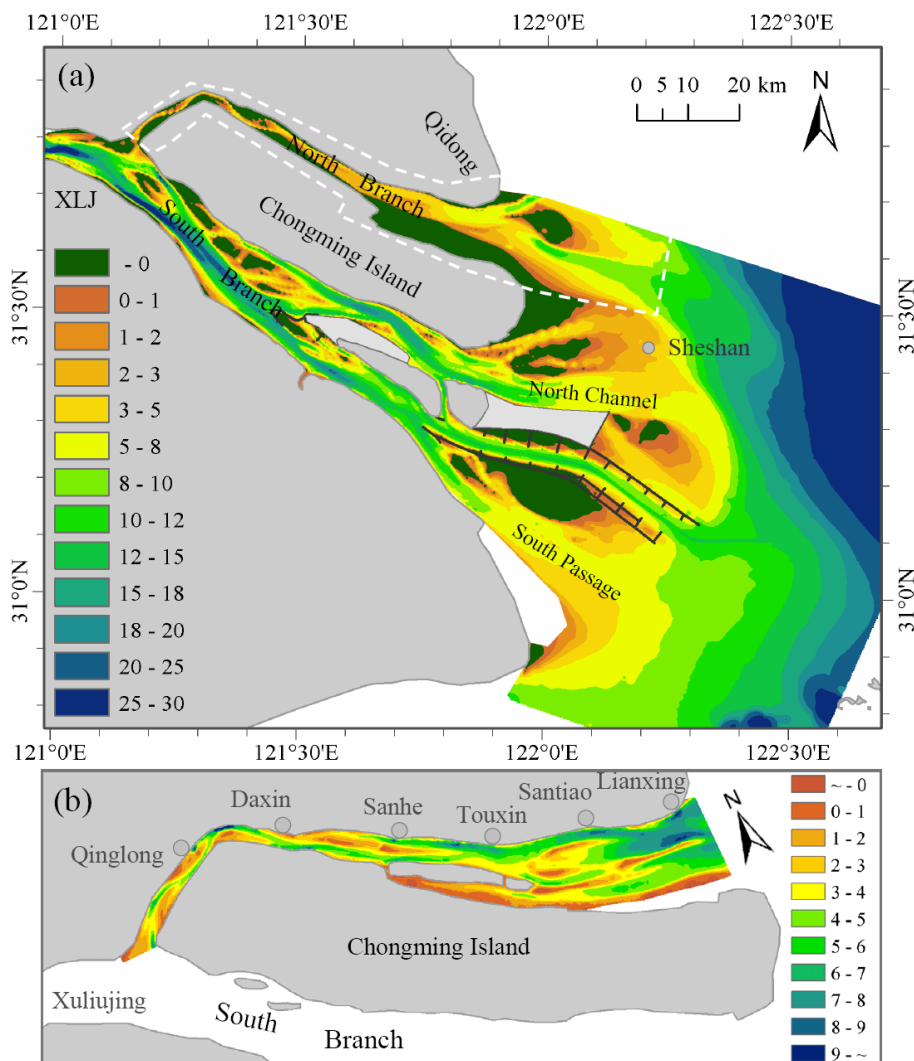
112 **2. Physical settings and data**

113 The Changjiang Estuary is one of the world's largest tidal estuaries in
114 terms of the magnitude of river discharge, strength of the tide, and spatial
115 scale of the tidally influenced reach. It is forced by a river discharge of
116 10,000–60,000 m³/s seasonally at the tidal wave limit and semi-diurnal tides
117 with a spring tidal range up to 5.9 m. Wind and wave effects and alongshore
118 currents are also significant but of secondary importance compared with rivers
119 and tides. The Changjiang Estuary is dynamically divided into a tidal river
120 upstream of Jiangyin where river forcing dominates, and a seaward tidal
121 estuary, where both the river and tides are important (Guo et al., 2015). The
122 tidal estuary has a funnel-shaped planform, and morphologically, it features by
123 three bifurcations into four main branches entering the East China Sea (Figure
124 1a).

125 The division between the North Branch and South Branch formed as a
126 result of the first bifurcation, and the latter is presently the major conduit of
127 river-borne freshwater and sediment. The South Branch and its seaward
128 channels have been scientifically examined in much more detail than the North
129 Branch owing to the importance of the former for navigation and water supply.
130 However, saltwater intrusion in the North Branch could reach the South Branch
131 and threatens the freshwater intake and supply for the reservoir surrounding
132 the South Branch (Wu et al., 2006). The strong saltwater intrusion is explained
133 by sub-tidal sea water accumulation in the upper part of the North Branch
134 because of converged Stokes' transport in response to channel narrowing
135 (Zhang et al., 2020). To mitigate saltwater intrusion, there is a plan to construct
136 a barrier (with gates) at the mouth of the North Branch, but the impact on the
137 ecosystem and the fate of the North Branch remains open questions.

138 The present North Branch is a convergent tide-dominant branch with minor
139 river influence (Figure 1b). Its upper part, from the inflow section to the bend
140 around Qinglong, has a length of 20 km, which is relatively narrow in width, i.e.,
141 a mean bankfull width of ~2.0 km. The middle and lower parts, downward the
142 bend until the mouth area, have a combined length of ~60 km, creating a

143 funnel-shaped channel with a high convergence rate. The branch width
 144 increases to ~12 km at the mouth section around Lianxing. The North Branch
 145 is shallower than other branches in the Changjiang Estuary, with a mean depth
 146 of 2–4 m (Dai et al., 2016), as a result of sediment import and intensive
 147 sedimentation over the past century. The mean tidal range at the mouth is 3.2
 148 m, and it increases up to 3.8 m in the middle segment and then decreases to
 149 2.6 m in the inflow section. Tidal bores are observed in the upper part of the
 150 North Branch owing to strong wave amplification, and the maximum tidal range
 151 is 5.0 m (Chen, 2003). Elongated tidal sand ridges developed in the lower part
 152 of the branch, and a mouth bar formed in the region seaward of the mouth.



153
 154 **Figure 1.** (a) The tidal estuary part of the Changjiang Estuary with its
 155 bathymetry in 2016; (b) the North Branch with its bathymetry in 1998. XLJ is

156 the abbreviation of Xuliujing. The water depth and elevations reference to the
157 lowest tides.

158

159 We collected data in the form of historical maps showing the large-scale
160 topography of the delta, instrumental bathymetry data of the North Branch
161 detailing the underwater morphology, and satellite images. Historical maps
162 published since the 17th century were collected to illustrate the planform
163 changes throughout the estuary and in the North Branch (see sections 3.1 and
164 3.2). The majority of the historical maps were collected from the University of
165 Texas library (<http://legacy.lib.utexas.edu/maps/historical/>), the Virtual
166 Shanghai website (<https://www.virtualshanghai.net>), the David Rumsey Map
167 Collections (<https://www.davidrumsey.com>), and the United States Library of
168 Congress (<https://www.loc.gov>), unless otherwise specified. Digitized
169 bathymetric data from 1958, 1978, 1998, and 2019 were geo-referenced and
170 analysed in-depth using GIS tools (see section 3.3). Satellite images captured
171 since 1974 were collected from Landsat (<https://earthshots.usgs.gov>), and
172 historical coastline changes were identified based on the dikes and levees.

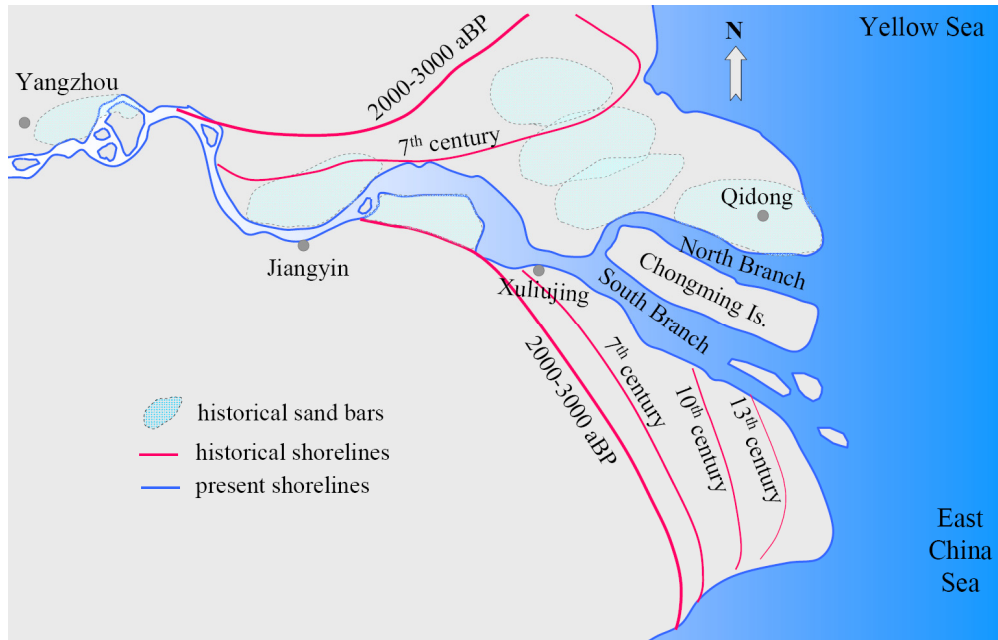
173

174 **3. Hydro-morphodynamic evolution**

175 **3.1 Initial branch bifurcation**

176 The initial formation of the North Branch is part of the development story of
177 the entire Changjiang delta. The development of the present sub-aerial delta
178 started from the infilling of an incised valley seaward of Yangzhou formed
179 during the low sea-level conditions (Figure 2; Chen et al., 1985). The present
180 delta began to prograde eastward when rising sea levels reached a height
181 close to present levels, which was around 6000–7,500 aBP (Wang et al., 2018).
182 The tides play a role in enhancing sediment deposition (Uehara et al., 2002).
183 Several sand bars and shoals successively developed in the river valley
184 (Figure 2; Chen et al., 1979; Li et al., 2002), which later developed into large
185 shoals and/or merged into the northern delta plain (Li et al., 2000, 2002; Zhang

186 and Meng, 2009; Jiang et al., 2020). The distributary channels over the delta
187 then moved south-eastward step-by-step with an infilled valley and delta
188 build-up (Figure 2).



189
190 **Figure 2.** A sketch of the historical development of the Changjiang River delta
191 over the past 2,000 years, with identified historical coastlines and sand bars
192 Adopted from Chen et al. (1985).

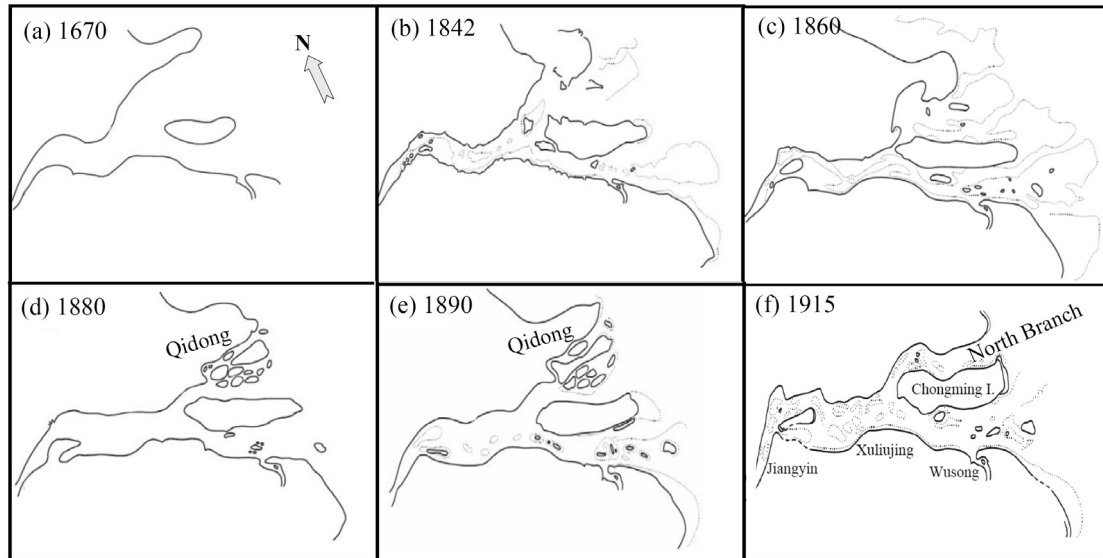
193
194 The sand bars scattered throughout the estuary changed profoundly in
195 size and location owing to channel migration, and no stabilized channels were
196 identified prior to the 7th century owing to alternating erosion and deposition
197 processes. Thereafter, several small mid-channel sand bars were combined to
198 produce one large sand bar, which formed the base of the present Chongming
199 Island. Starting from the 7th century, human settlements on the sand bars and
200 other human activities helped to stabilize the coastlines of this island (Chen et
201 al., 1979, 1985). The stabilized Chongming Island then led to a stable
202 bifurcation between the South Branch and the North Branch.

203
204 **3.2 Stabilized development**

205 Field data of the North Branch are rare prior to the 1950s, and the

206 morphological evolution of this branch is interpreted mainly based on historical
207 geography maps and geological studies. The North Branch was a main
208 distributary channel flushing a major portion of fluvial water and sediment to
209 the sea prior to the 1860s (Yun, 2004), with a sub-tidal flow partition rate (i.e.,
210 the ratio of the tide-averaged flow towards the North Branch compared to the
211 total of North and South branches) exceeding 50%. Deposition of
212 river-supplied sediment within the North Branch caused rapid development of
213 the northern delta plain and an overall south-eastward realignment of the
214 entire delta (Figure 3). As a result, the majority of the fluvial water and
215 sediment has been diverted into the South Branch since the 19th century, and
216 the North Branch has since become a secondary distributary channel (Chen
217 and Li, 2002).

218 Historical maps reveal the planform changes in a straightforward manner,
219 although they lack details of the underwater bathymetry (Figures 3 and S1–S2).
220 The initial North Branch was fairly wide and appeared to be a sub-basin rather
221 than a branch; it was initially called the North Entrance following its formation.
222 Continued sedimentation led to the development of a series of sand bars and
223 shoals inside the North Branch. In the late 19th century, the sand bars that
224 formed around the mouth section merged into the northern bank, resulting in a
225 profound south-eastward advance of the northern delta plain (i.e., eastward by
226 ~27 km and southward by ~15 km) between 1842 and 1912 (Figure 3; Yun,
227 2004). Since then, the changes along the northern coastline of the North
228 Branch became limited owing to shoreline protection activities. The inflow
229 section of North Branch had a width of 15 km, and the mouth section was 36
230 km in width in 1842 (Yun, 2004). However, the inflow segment narrowed
231 significantly after the 1860s due to the formation and merging of sand bars into
232 the northern bank, leading to a reduction in width to 5.8 km in 1915 (see Figure
233 4a).



234

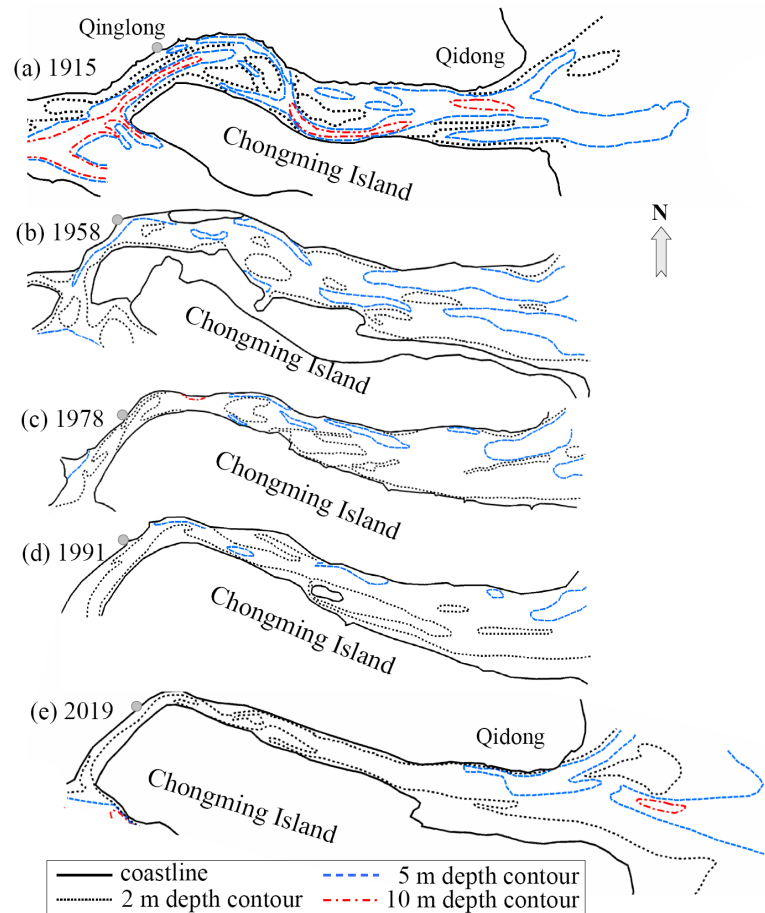
235 **Figure 3.** Planform changes of the Changjiang Delta and the North Branch in
 236 the past 300 years: (a) 1670, (b) 1842, (c) 1860, (d) 1880, (e) 1890, and (f)
 237 1915. Adopted from Huang (1986) and Yun (2004) and historical maps (see
 238 Figures S1 and S2).

239

240 More details regarding the underwater bathymetry are available in maps
 241 published in 1915–1917 (see Figure S2). The North Branch was nearly uniform
 242 in width at that time, although it had a curved planform (Figure 4a). The
 243 sub-tidal flow partition ratio reduced to approximately ~25% in 1915, which
 244 implies a significant fluvial influence (Zou, 1981; Chen et al., 1988).
 245 Meandering channels and sand bars developed inside the North Branch, and
 246 the overall channel-shoal configuration was consistent with the curved
 247 planform (Figure 4a). Deeper ebb channels developed toward the outer bends
 248 of the meanders while flood channels flanked the sand bars. In the mouth zone,
 249 sedimentation produced a mouth bar, and the ebb tidal delta grew larger over
 250 time. This channel-shoal pattern is typical of that in long tidal basins and
 251 estuaries (van Veen et al., 1950).

252 Beginning in 1958, the North Branch became much narrower,
 253 predominantly owing to strong sedimentation along the southern bank (Figure
 254 4b); however, the northern bank had also retreated by 2–3 km on average

255 between 1907 and 1958 (Zou, 1987; Yun, 2004). The width of the Qinglong
256 section decreased from 6 km in 1917 to 2 km in 1958, while that of the Sanhe
257 section decreased from 8.5 km in 1917 to 4.0 km in 1978 (Chen et al., 1985).
258 Convergence in planform started to emerge owing to more width reduction in
259 the upper regions of the branch. Moreover, the North Branch also became
260 shallower and the meandering channel-shoal structure vanished. Its sub-tidal
261 flow partition rate declined to ~7.6% in 1958 (Zou, 1987; Yun, 2004), implying a
262 decreased river influence and a change towards tide dominance. Tidal bores
263 began forming in the 1940s (Chen and Shen, 1988). In addition, the partition
264 rate of the sub-tidal flow was negative during the spring tides in the dry season
265 as early as 1959, suggesting a reversed flow and the occurrence of flood
266 dominance. Sediment import led to a net deposition of 1.45 km³ between 1915
267 and 1958 within the North Branch (Zou, 1987). Therefore, the previously
268 present meandering channel-shoal structure was replaced by disconnected
269 shallow tidal channels and elongated sand ridges (Figure 4).



270

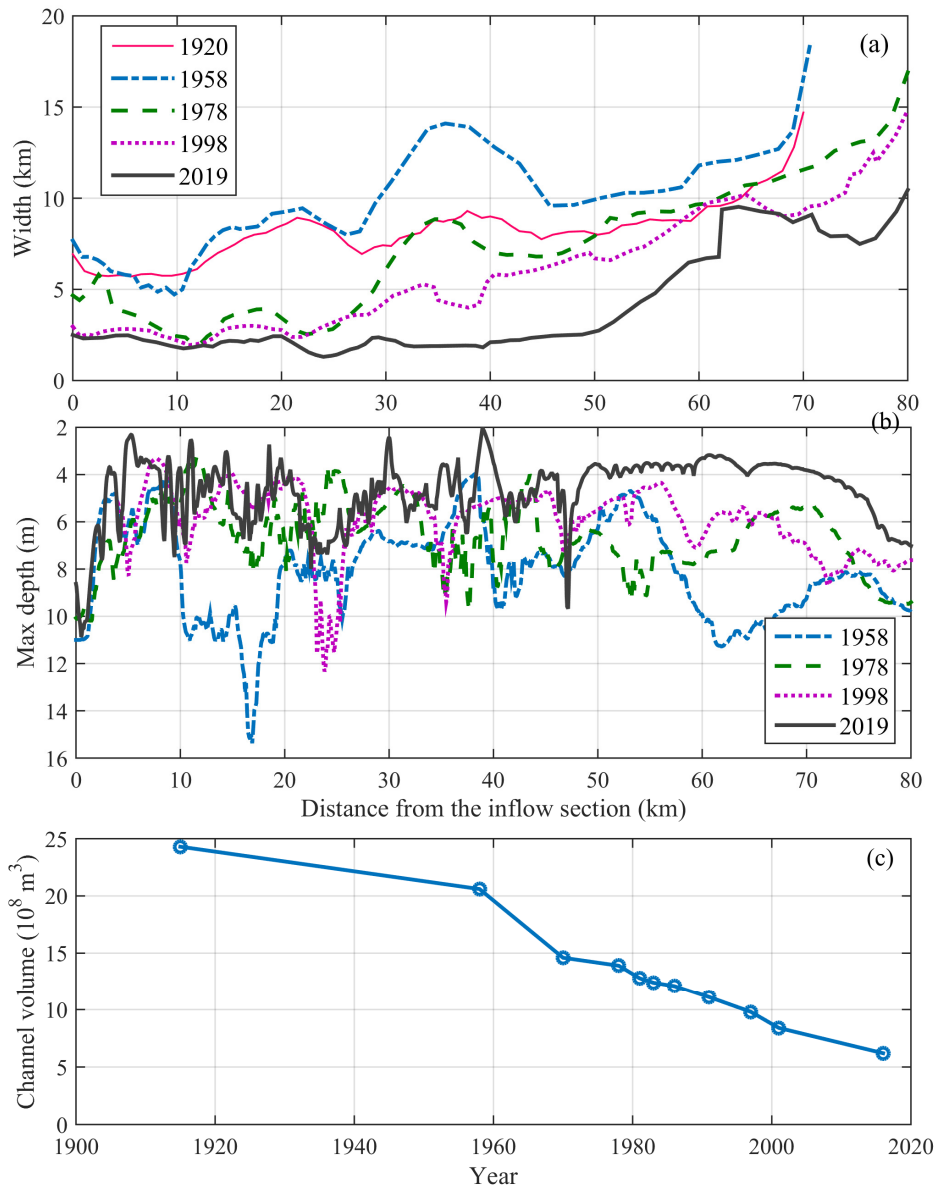
271 **Figure 4.** Sketches of the topography changes of the North Branch in (a) 1915,
 272 (b) 1958, (c) 1978, (d) 1991, and (e) 2019. Historical data prior to 1991 are
 273 acquired from Zou (1987) and Yun (2004).

274

275 3.3 Human-forced evolution

276 The hydro-morphodynamic evolution has accelerated since 1958 owing to
 277 increased human intervention. The Xuliujing section, the river reach that
 278 controls the division between the South and North branches, was narrowed
 279 due to the merging and diking of the sand bars along the northern bank during
 280 the 1970s–1990s. As a result, the inflow section of the North Branch was
 281 further narrowed as well, which substantially altered the inflow conditions and
 282 the tidal regime (Figures 4 and 5). Severe sedimentation occurred in the inflow
 283 segment of the North Branch due to tide-induced sediment trapping. Both
 284 changes reduced the cross-sectional area of the inflow section. The channel

285 alignment of the inflow segment developed nearly normal to the main branch
286 stretching from Xuliujing to the South Branch; this deteriorated inflow further
287 reduced the partition rate and fluvial influence on the North Branch. For
288 example, the flood current duration in the Qinglong section decreased from
289 ~4.5 hours in 1958 to ~3.6 hours in 1985 (Chen, 1994; Yun, 2004). The
290 sub-tidal flow partition ratio declined to 1–2% after the 1950s (e.g., it was 1.5%
291 in 1984) (Huang, 1986). The North Branch eventually became predominantly
292 tide-dominant with very limited river influence. The tides were strongly
293 amplified in the upper part of the North Branch, leading to the formation of tidal
294 bores. The mean tidal range increased by 0.25 m in 1978 compared with that
295 in 1958. The energetic flow conditions enhanced the suspended sediment
296 concentrations in the upper reaches (Yang et al., 2020), where the bottom
297 sediments were much sandier than those in the lower reaches.



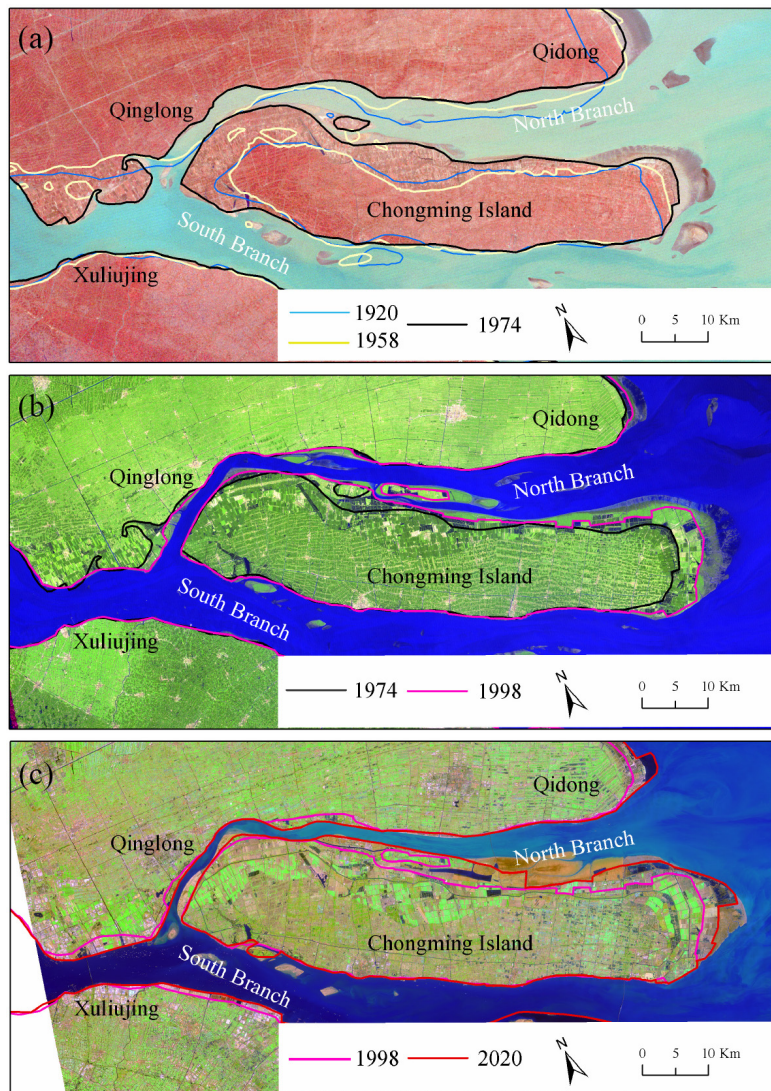
298

299 **Figure 5.** Changes in the (a) channel width at the mean water level, (b)
 300 cross-sectional averaged depth (referencing to the lowest tide), and (c)
 301 channel volume below the mean water level in the North Branch. Historical
 302 data of the channel volume in panel (c) are acquired from Zhang and Cao
 303 (1998) and Yun (2004, 2010).

304

305 The infill of the North Branch continued in the 1980s, as depicted in the
 306 satellite images available since 1974 (Figure 6). The narrowing trend
 307 continued in the upper and middle reaches, as the shoals formed close to the
 308 southern bank were reclaimed, merging into Chongming Island. The length of

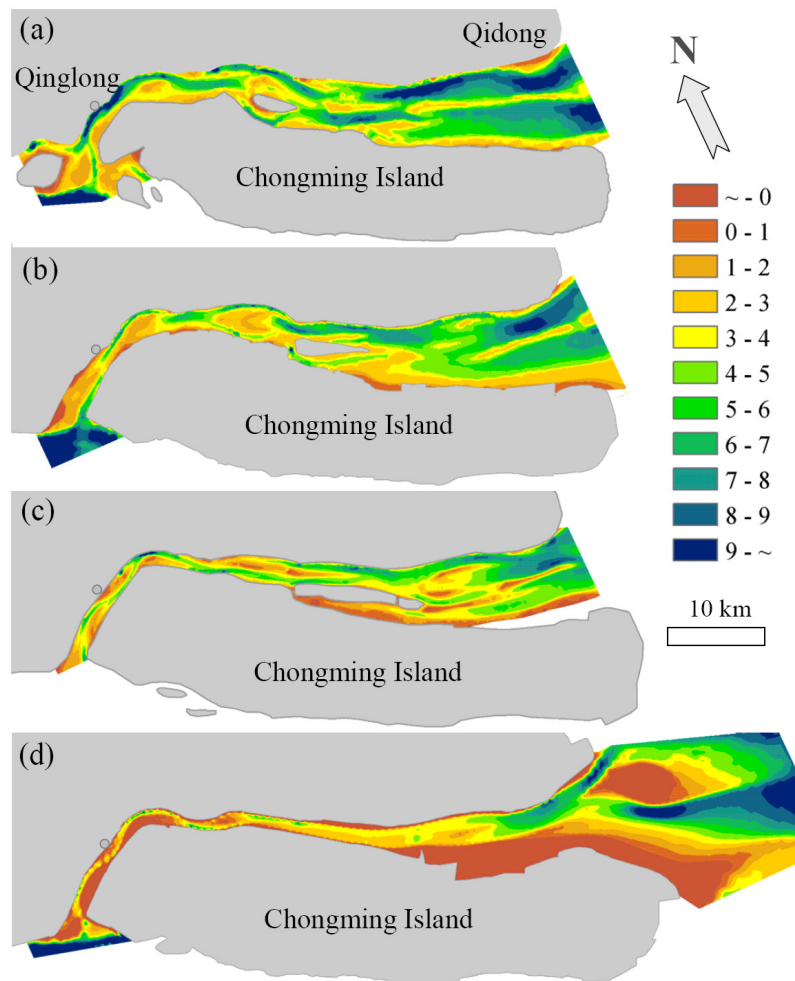
309 the North Branch increased slightly because of the seaward advance of the
310 Qidong spit and southern Chongming Island (see Figure 5a). The surface
311 planform area of the North Branch declined by 51% over ~60 years, i.e., from
312 $\sim 6.9 \times 10^7 \text{ m}^2$ in late 1958 to $\sim 5.5 \times 10^7 \text{ m}^2$ in 1984 and $\sim 3.4 \times 10^7 \text{ m}^2$ in 2019. As
313 of 2019, the narrowest inflow section was $< 2 \text{ km}$ in width and that of the mouth
314 section was 7.5 km .



315
316 **Figure 6.** Satellite images of the North Branch in (a) 1974, (b) 1998, and (c)
317 2020 (during high tide), together with the identified coastlines. The shorelines
318 in 1920 and 1958 were obtained from historical maps (see Figure S2).

319
320 More readily available bathymetric data since 1958 enabled the
321 quantification of changes in the tidal flat area and channel volume (Figure 7).

322 The northern bank of the North Branch underwent erosion and a shoreline
323 retreat of 1.7–2.6 km on average between the 1950s and 1980s (Chen et al.,
324 1985). Thereafter, the northern shorelines were protected with dikes, and the
325 shoreline retreat ceased. The southern bank of the North Branch advanced by
326 ~4.5 km on average between 1900 and 1998. The length of the branch was
327 increased by approximately 10 km in response to the advanced northern delta
328 plain and the expansion of Chongming Island during 1958–2019 (Figure 6).
329 However, the surface area of the North Branch decreased from 6.9×10^7 m² in
330 1958 to 3.4×10^7 m² in 2019. The channel width at the inflow section decreased
331 from ~5.1 km in 1958 to 2.5 km in 2019, while the width of the mouth section
332 decreased from ~15 km to ~7.5 km accordingly (Figure 5a). In addition, the
333 maximum depth decreased from 11 m in 1907 to 7 m in 1958 and 5.8 m in
334 1991 (Zhang and Cao, 1998), while the mean depth of the branch decreased
335 from 5.3 m in 1958 to 3.5 m in 2019. This indicates a significant shoaling trend
336 (Figure 5b). The channel volume below the 0 m contour (referencing to the
337 lowest tide, which indicates the sub-tidal channel volume) decreased from
338 2.90×10^9 m³ in 1958 to 1.54×10^9 m³ in 1978 and 0.67×10^9 m³ in 2019 (see
339 Figure 5c), as a result of the combined influence of channel infilling and width
340 reduction. Compared with the situation in 1915, the majority of the channel
341 volume reduction occurred prior to 1958. Accordingly, the mean sedimentation
342 rate within the North Branch was 33.8×10^6 m³ yr⁻¹ between 1915 and 1958
343 (Huang, 1986; Zou, 1987); it increased to 46.0×10^6 m³ yr⁻¹ during 1958–1978,
344 73.8×10^6 m³ yr⁻¹ during 1978–1998, and to 83.0×10^6 m³ yr⁻¹ during 1998–2019.
345 This suggests an increased sedimentation rate over time.



346

347 **Figure 7.** Bathymetry of the North Branch in (a) 1958, (b) 1978, (c) 1998, and
 348 (d) 2019. The depth is relative to the lowest tide.

349

350 **4. Discussion**

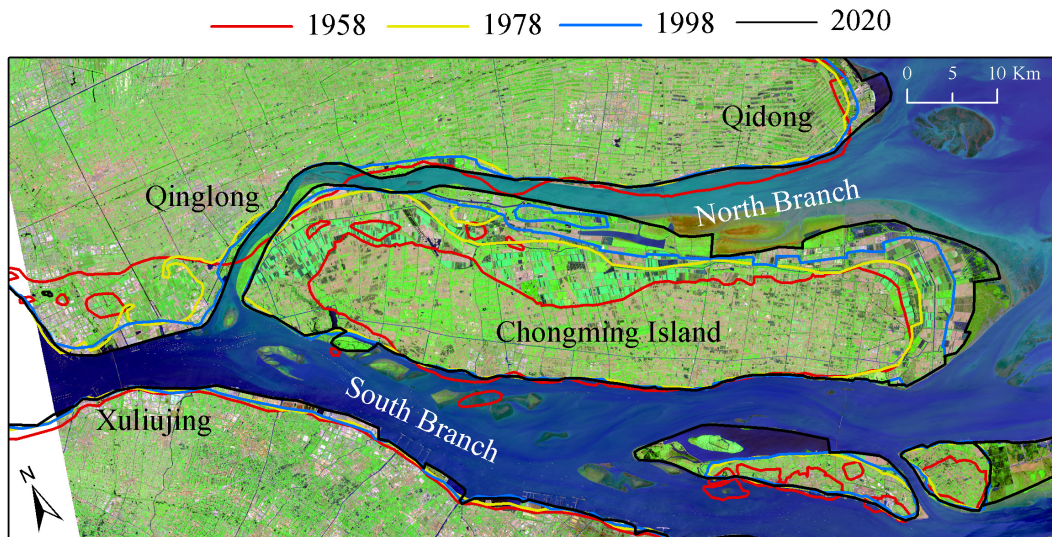
351 **4.1 Impact of human activities**

352 Human activities have played an important role in modulating the
 353 hydro-morphodynamics in the North Branch, particularly since the 1950s. The
 354 river-supplied sediment to the estuary has declined since the mid-1980s owing
 355 to hydropower dams and reforestation measures in the watershed (Guo et al.,
 356 2019), but its impact on the North Branch is thus far limited given its
 357 tide-dominant nature. Engineering projects in other parts of the estuary, e.g.,
 358 the navigation channel regulation plans in the North Passage (see Figure 1a),
 359 are not expected to have direct influence on the North Branch either. The main
 360 type of human intervention is diking and reclamation of the sand bars and tidal

361 flats surrounding the North Branch; activities such as dredging and barrier
362 construction are rare (Figure 8). Human settlement on Chongming Island since
363 the 7th century has enhanced the bifurcation between the North and South
364 branches. Shoreline protection by dikes along the northern bank has
365 prevented its erosion since the 1970s. Additionally, reclamation of the sand
366 bars and shoals around the Xuliujing section between 1958 and 1972
367 narrowed the inflow segment (Chen and Li, 2002), resulting in a significant
368 decline of its sub-tidal flow partition ratio.

369 In addition, the embankment of sand bars and tidal flats along the southern
370 bank has played a substantial role in altering channel convergence. Since
371 1954, the northern bank close to the Qinglong section has been protected from
372 erosion by dikes. A series of sand bars that formed in the middle segment of
373 the North Branch, e.g., the Yonglong, Xinglong, and Huanggua shoals, have
374 been reclaimed successively since the 1970s and have merged into the
375 southern bank. The upper and middle segments significantly narrowed
376 between 1915 and 1970, and the narrowing mainly occurred in the middle and
377 lower parts of the branch since the 1970s. In the past 50 years, the cumulative
378 reclamation area along the bank of the North Branch has been about ~940 km²,
379 which explains the significant reduction in the surface area (Figure 8).

380 Overall, extensive tidal flat embankment has profoundly reduced the
381 bankfull channel width and surface area of the North Branch. The width
382 reduction was much more significant in the upper and middle reaches, which
383 enhances the width convergence. Subsequently, the incoming tidal waves
384 were more amplified, and the associated tidal asymmetry led to flood
385 dominance and sediment import. Human activities have likely played a
386 substantial role in accelerating the aggradation of the North Branch since the
387 1950s, when it became tide-dominant.



388
 389 **Figure 8.** Illustrated coastline changes of the North Branch between 1958 and
 390 2020 based on a satellite image obtained during a low tide in May 2020.

391
 392 **4.2 Causes of the regime shift**

393 The centennial morphodynamic evolution of the North Branch features
 394 channel shrinkage and a regime shift. In the period prior to 1915, the fluvial
 395 influence was still significant in supplying sediment and flushing sediment
 396 seaward in the wide North Branch. Between 1915 and 1958, the sand bars
 397 around the inflow and outflow segments merged into the northern delta plain
 398 and the configuration of the North Branch became more funnel-shaped with a
 399 profoundly reduced river influence and partition rate compared with that of the
 400 South Branch. Tides became strongly amplified (see Figure S4) and became
 401 the primary forcing condition initiating sediment trapping. Since 1958,
 402 intensified human interferences in terms of tidal flat reclamation has further
 403 enhanced the channel convergence, which has possibly resulted in
 404 accelerated sedimentation. Because of the deteriorated inflow configuration, a
 405 shift from a river-tide mixed influence towards tide and flood dominance
 406 occurred when the sub-tidal flow partition ratio decreased to <5% since the
 407 1950s.

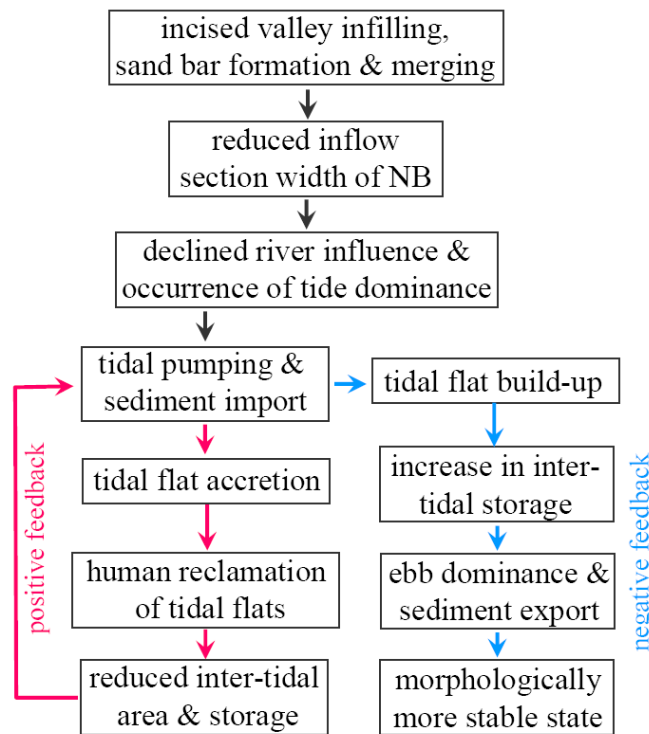
408 The regime shift from ebb to flood dominance is the combined result of the
 409 natural morphodynamic adaptation of the delta and human interference. Under

410 the combined strong river and tidal forcing, the distributary channels migrated
411 southeastward, while the sand bars and shoals moved north-westward. The
412 sand bars also underwent erosion to the south-east side and sedimentation to
413 the northwest side (Chen et al., 1985). This large-scale behaviour is ascribed
414 to the influence of incoming oceanic tidal waves from the south-east, the
415 Coriolis force (which favours channel realignment to the right-hand side in the
416 northern hemisphere), and the southward alongshore currents. This natural
417 trend is in line with the observed accretion along the southern bank and
418 erosion of the northern bank within the North Branch. In addition, this pattern is
419 also believed to facilitate the development of the distributary branches to the
420 south of the delta and the degeneration of the branch to the north. This
421 large-scale pattern of deltaic channel adjustment may explain the
422 sedimentation and fate of the North Branch on the longer term.

423 As the inflow section continued to narrow and the sub-tidal flow partition
424 rate decreased, the amplified tides continued to dominate over the fluvial
425 influence. The tide-dominant environment leads to a shorter rising tide duration,
426 stronger flood currents and associated sediment import and channel infilling
427 (see Figure S5). The rising tide duration was 5.4 hours at the mouth and
428 decreased to 3.1 hours at Qinglong based on data between 1988 and 2001
429 (Yun, 2004). It benefits larger flood currents and the development of flood
430 dominance and sediment import (Figure S5). Other than the seaward residual
431 sediment transport in the utmost reaches landward of the Qinglong section
432 owing to the remaining river influence, landward residual sediment transport
433 dominated in the middle and lower parts of the branch owing to strong tidal
434 asymmetry (Yang and Liu, 2002). The convergence of residual sediment
435 transport explains strong sedimentation and shoaling in the upper reaches.
436 Such shoaling persists until today, as indicated by the development of tidal
437 flats that are not submerged even during high tide (see Figure 6c). The
438 formation of the tidal flats in the inflow section tends to reduce the channel
439 width to <1 km therein. In the lower reaches, although the sediments imported

440 into the North Branch are derived from the sea side, these sediments mainly
 441 originate from the Changjiang River that are flushed to the nearshore region
 442 through the North Channel, which are then pumped into the North Branch by
 443 the tides (Shi et al., 1985; Chen and Li, 2002).

444 Human activities play a role in accelerating the regime shift by reducing the
 445 inflow section width and inter-tidal hydraulic storage over inter-tidal areas,
 446 enhancing the channel convergence, and stabilizing the channel configuration
 447 (see section 4.1). Moreover, progressive tidal flat reclamation following the
 448 establishment of tide dominance may initiate a positive feedback process
 449 (Figure 9). Inter-tidal flats favour the development of ebb dominance owing to
 450 their hydraulic storage effect; in contrast, tidal flat reclamation and the
 451 subsequent loss of tidal flat areas and storage volumes is to the advantage of
 452 flood dominance and sediment import. Sediment import stimulates tidal flat
 453 accretion and development, which attracts more reclamation and in turn
 454 enhances sediment import. This positive feedback explains the progressive
 455 and persisting sedimentation and infilling of the North Branch in the most
 456 recent half century (Figure 9).



457

458 **Figure 9.** A conceptual diagram of the positive feedback between

459 human-initiated tidal flat embankments and sediment import in the North
460 Branch, and a possible negative feedback when tidal flat reclamation ceases.

461

462 It is worthwhile to note that ebb dominance and net sediment export may
463 occur in tide-dominant estuaries. For instance, van der Wegen et al. (2008)
464 have modelled ebb dominance in a schematized tidal basin with a similar size
465 to that of the North Branch; the ebb dominance was ascribed to the impact of a
466 seaward Stokes' return flow and inter-tidal flats. We believe that the
467 occurrence of flood dominance and sediment import in the North Branch is the
468 result of a limited fluvial influence owing to a small partition rate and the
469 development of a highly convergent planform which substantially amplifies the
470 tides. The tides are dominant over the river influence and hydraulic impact of
471 little inter-tidal flats. High sediment availability from the Changjiang River and
472 the nearshore regions may also contribute to the persistent sediment import.
473 Further in-depth examination of the mechanisms governing the flood
474 dominance and its spatio-temporal variations using a numerical model will be
475 performed in a future study.

476

477 **4.3 Water resource and ecological management perspectives**

478 Flood dominance and the associated sediment import have been detected
479 in many tidal basins and estuaries worldwide, which is considered to be
480 beneficial for water resource and ecological management given the worldwide
481 sediment deficiency and sea-level rise. For instance, sediment budget analysis
482 has indicated a net sediment import in the Humber Estuary in the U.K.,
483 predominantly owing to a low river flow and strong tidal asymmetry that pumps
484 mud into the estuary (Townend and Whitehead, 2003). In the Dutch Wadden
485 Sea, persistent sediment import through multiple tidal inlets helps to restore
486 tidal flats, which counteracts the inundation impact of sea-level rise (Wang et
487 al., 2018). The flood dominance and sediment import in the North Branch in
488 this case, however, necessitate mitigation, because too strong a sediment

489 import process results in fast channel aggradation and loss of channel volume,
490 which raises concerns on its disconnection from the remaining parts of the
491 estuary.

492 There are multiple objectives to be considered in the integrated
493 management of the North Branch. The shallow water and tidal flats provide
494 important habitats for birds and fish and associated valuable ecosystem services.
495 The saltwater intrusion into the South Branch threatens the function of the
496 reservoirs that supply freshwater resources for >10 million people in Shanghai.
497 The North Branch also provides a waterway for small boat shipping and
498 accommodates sewage from the factories and industries surrounding the
499 branch. A big concern is that continued sediment import may lead to severe
500 aggradation of the North Branch in the medium to long term. Such changes
501 would mitigate saltwater intrusion but indicate a loss of a connected branch
502 with significant ecosystem value and as a drainage channel for the
503 surrounding cities. There is a plan to build a barrier with gates at the mouth of
504 the North Branch to regulate tidal intrusion and sediment flushing, but no
505 consensus has been achieved thus far regarding its potential impact on the
506 ecosystem or the estuary as a whole.

507 Authorities much protect the branch from continuous aggradations while
508 simultaneously alleviating the impact of saltwater intrusion and preserving the
509 wetlands. Considering the positive feedback impact of tidal flat reclamation,
510 one management option is to cease tidal flat embankment and allow the tidal
511 flats to build up naturally inside the branch. Once the inter-tidal flat area and
512 storage volume are restored, the flood dominance and sediment import may
513 decline, and a morphodynamic equilibrium may be established. One remaining
514 question is at what time scale the branch is likely to be restored to equilibrium,
515 considering no additional anthropogenic interference. A decline in sediment
516 availability from the Changjiang River is likely to prolong this adaptation time
517 scale.

518 The embankment of tidal flats and the construction of dikes have long

519 been used as effective measures in protecting coasts from erosion and
520 flooding. However, because of high maintenance costs and the low but
521 possible risk of infrastructure failure under episodic catastrophic events, it
522 becomes increasingly clear that sustaining waterfront tidal flats and salt
523 marshes is beneficial for both coastal and ecosystem protection (Temmerman
524 et al., 2013). While delta land has increased globally (Nienhuis et al., 2020),
525 global tidal flats have decreased as a result of human-initiated reclamation
526 (Murray et al., 2019). A mindset change from hard engineering projects (e.g.,
527 dikes and groins) to soft eco-engineering (e.g., salt-marshes and similar
528 ecological measures) is occurring in the coastal management community.
529 Management that allows for nature to adjust and adapt to external changes
530 such as managed retreat also increase the system's resilience to floods and
531 sea-level rise (Townend and Pethick, 2002; Temmerman et al., 2003).
532 Abandoning tidal flat embankment would likely be of similar value for long-term
533 stability and resilience in the North Branch, particularly when considering a
534 decline in suspended sediment concentrations and sediment availability on the
535 marine side (Yang et al., 2020).

536

537 **5. Conclusions**

538 In this study, we revisited the centennial hydro-morphodynamic evolution
539 of the North Branch, a bifurcated branch in the fluvio-deltaic Changjiang
540 Estuary, based on a literature review and reanalysis of historical maps, satellite
541 images and bathymetric data. We see that the North Branch was once a major
542 distributary branch (sub-tidal flow partition >50%) and then became a
543 secondary branch with a sub-tidal flow partition rate reduced to ~25% in 1915,
544 when it was still ebb-dominant and developed alternative meandering
545 channels and sand bars that are typical of tidal estuaries. Continuous
546 deposition of river-borne sediment leads to a narrowing of the branch,
547 particularly in the outflow regions where the northern delta plain advanced
548 quickly. In the inflow regions, human-initiated reclamation of tidal flats reduced

549 the bankfull width and modified the channel configuration. Its sub-tidal partition
550 rate has reduced to <5% since the late 1950s, and since then the North Branch
551 became funnel-shaped in planform and tide- and flood-dominant under forcing
552 conditions, in which tidal bores and sand ridges developed.

553 We argue that the regime shift and aggradation of the North Branch are a
554 combined result of natural evolution and human activities. The south-eastward
555 realignment of the entire delta leads to abandonment of the distributary
556 channels to the north, e.g., the North Branch. As the sub-tidal flow partition rate
557 decreases below a threshold, the strongly amplified tides dominate over the
558 fluvial influence, leading to the establishment of tide dominance. Subsequent
559 tidal asymmetry then induces flood dominance and sediment import, while
560 subsequent human activities in terms of extensive tidal flat reclamation
561 accelerate the changes by reducing the channel width and increasing channel
562 convergence. A positive feedback process is identified between
563 human-initiated flat embankment and enhanced sediment import, which
564 explains the persisting sediment import in the past century. Management of the
565 North Branch must be performed considering the interactions among different
566 branches within the delta as a whole. We believe that abandoning aggressive
567 tidal flat reclamation may help to restore tidal flats which would mitigate
568 sediment import and channel aggradation on the longer term. Further
569 exploration of the regime changes and governing mechanisms will be
570 presented in an accompanying paper when using a numerical modelling tool.

571

572

573 **Acknowledgements**

574 This work is supported by the project 'Coping with deltas in transition' within
575 the Programme of Strategic Scientific Alliance between China and The
576 Netherlands (PSA), financed by the Ministry of Science and Technology, P.R.
577 China (MOST) (No. 2016YFE0133700) and Royal Netherlands Academy of
578 Arts and Sciences (KNAW) (No. PSA-SA-E-02), and also partly by MOST (No.

579 2017YFE0107400), Natural Science Foundation of China (Nos. 51739005,
580 U2040216, 41876091), and Shanghai Committee of Science and Technology
581 (Nos. 18DZ1206400; 19QA1402900; 20DZ1204700).

582

583 **References**

584 Chen B.C., 1994. The change of the general form and the transport of the
585 water, load and salt about the North Branch of the Changjiang River mouth.
586 Chinese Geographical Science 4(3), 242-251.

587 Chen J.Y., Yun C.X., Xu H.G., Dong Y.F., 1979. The developmental model of
588 the Changjiang River estuary during the last 2000 years. *Acta Oceanologia*
589 *Sinica* 1, 103-111.

590 Chen J.Y., Li D.J., 2002. Regulation of the Changjiang Estuary: past, present
591 and future. In: Chen J.Y., Eisma D., Hotta K., and Walker H.J. (eds.),
592 *Engineered Coasts*, Kluwer Academic Publishers, Netherlands, pp. 185-197.

593 Chen J.Y., Shen H.T., 1988. Some key point on harnessing the Changjiang
594 estuary. In: *Processes of Dynamics and Geomorphology of the Changjiang*
595 *Estuary*. Shanghai Scientific and Technical Publishers. pp. 419-423 (in
596 Chinese).

597 Chen J.Y., Zhu H.F., Dong Y.F., Sun J.M., 1985. Development of the
598 Changjiang Estuary and its submerged delta. *Continental Shelf Research* 4,
599 47-56.

600 Chen S.L., 2003. Tidal bore in the North Branch of the Changjiang Estuary. In
601 *Proceedings of the International Conference on Estuaries and Coasts*,
602 Hangzhou, China. pp, 233-239.

603 Chen Z.Y., Stanley D.J., 1998. Sea-level rise on eastern China's Yangtze Delta.
604 *Journal of Coastal Research* 14, 360-366.

605 Dai Z.J., Fagherazzi S., Mei X.F., Chen J.Y., Meng Y., 2016. Linking the infilling
606 of the North Branch in the Changjiang (Yangtze) estuary to anthropogenic
607 activities from 1958 to 2013. *Marine Geology* 349, 1-12.

608 de Vriend H.J., Wang Z.B., Ysebaert T., Herman P.M.J., Ding P.X., 2011.

609 Eco-morphological problems in the Yangtze Estuary and the Western Scheldt.
610 Wetlands, doi:10.1007/s13157-011-0239-7.

611 Dronkers J., 1986. Tidal asymmetry and estuarine morphology. Netherland
612 Journal of Sea Research 20(2/3), 117–131.

613 Guo L.C., Su N., Townend T., Wang Z.B., Zhu C.Y., Zhang Y.N., Wang X.Y., He
614 Q., 2019. From the headwater to the delta: A synthesis of the basin-scale
615 sediment load regime in the Changjiang River. Earth-Science Reviews 197,
616 102900, doi.org/10.1016/j.earscirev.2019.102900.

617 Guo L.C., van der Wegen M., Roelvink J.A., He Q., 2014. The role of river flow
618 and tidal asymmetry on 1D estuarine morphodynamics. Journal of
619 Geophysical Research: Earth Surface 119, 2315-2334, doi:
620 10.1002/2014JF003110.

621 Guo L.C., van der Wegen M., Jay D.A., Matte P., Wang Z.B., Roelvink J.A., He
622 Q., 2015. River-tide dynamics: exploration of nonstationary and nonlinear
623 tidal behavior in the Yangtze River estuary. Journal of Geophysical Research:
624 Oceans 120, doi:10.1002/2014JC010491.

625 Friedrichs C.T., Aubrey D.G., 1988. Non-linear tidal distortion in shallow
626 well-mixed estuaries: a synthesis. Estuarine, Coastal and Shelf Science 27,
627 521-545.

628 Huang S., 1986. The evolution characteristics of the Changjiang Estuary.
629 Journal of Sediment Research 4, 1-12.

630 Jiang F., Zhao X.S., Chen J., Liu Y., Sun Q.L., Chen J., Chen Z.Y., 2020.
631 Depocenter shift and en-echelon shoal development in the pre-holocene
632 incised valley of the Yangtze Delta, China. Marine Geology,
633 doi.org/10.1016/j.margeo.2020.106212.

634 Lanzoni S., Seminara G., 1998. On tide propagation in convergent estuaries.
635 Journal of Geophysical Research 103(C13), 30793–30812.

636 Li C.X., Chen, Q.Q., Zhang J.Q., Yang S.Y., Fan D.D., 2000. Stratigraphy and
637 paleoenvironmental changes in the Yangtze Delta during the Late Quaternary.
638 Journal of Asian Earth Science 18, 453–469.

639 Li C.X., Wang P., Sun H.P., Zhang J.Q., Fan D.D., Deng B., 2002. Late
640 quaternary incised-valley fill of the Yangtze Delta (China): its stratigraphic
641 framework and evolution. *Sedimentary Geology* 152, 133-158.

642 Li X., Zhang X., Qiu C.Y., Duan Y.Q., Liu S.A., Chen D., Zhang L.P., Zhu C.M.,
643 2020. Rapid loss of tidal flats in the Yangtze River Delta since 1974.
644 *International Journal of Environmental Research and Public Health* 17, 1636,
645 doi:10.3390/ijerph17051636.

646 Liu F., Xie R.Y., Luo X.X., Yang L.Z., Cai H.Y., Yang Q.S., 2019. Stepwise
647 adjustment of deltaic channels in response to human interventions and its
648 hydrological implications for sustainable water management in the Pearl
649 River Delta, China. *Journal of Hydrology* 573, 194-206.

650 Nienhuis J.H., Ashton A.D., Edmonds D.A., Hoitink A.J.F., Kettner A.J.,
651 Rowland J.C., Tornqvist T.E., 2020. Global-scale human impact on delta
652 morphology has led to net land area gain. *Nature* 577, 514-518.

653 Meng Y., Cheng J., 2005. The atrophy of the estuarine North Branch of the
654 Yangtze River (Changjiang River). *Marine Geology Letters* 21(1), 1-10. (in
655 Chinese)

656 Murray N.J., Phinn S.R., DeWitt M., Ferrari R., Johnston R., Lyons M.B.,
657 Clinton N., Thau D., Fuller R.A., 2019. The global distribution and trajectory
658 of tidal flats. *Nature* 565, 222-225.

659 Obodoefuna D.C., Fan D.D., Guo X.J., Li B., 2020. Highly accelerated siltation
660 of abandoned distributary channel in the Yangtze Delta under everchanging
661 social-ecological dynamics. *Marine Geology* 429, 106331,
662 <https://doi.org/10.1016/j.margeo.2020.106331>.

663 Pethick J.S., 1994. Estuaries and wetlands: function and form. In: *Wetland*
664 *Management*, Thomas Telford, London, pp. 75-87.

665 Ridderinkhof W., de Swart H.E., van der Vegt M., Alebregtse N.C., Hoekstra P.,
666 2014. Geometry of tidal inlet systems: A key factor for the net sediment
667 transport in tidal inlets. *Journal of Geophysical Research: Oceans* 119 (10),
668 6988-7006, doi: 10.1002/2014jc010226.

669 Shi L.R., Wei T., Shen H.S., 1985. The diffusion of seaward sediments from
670 Yangtze River and the source of depositing sediments in the North Branch.
671 Journal of Yangtze River Scientific Research Institute 2, 8-19.

672 Speer P.E., Aubrey D.G., 1985. A study of non-linear tidal propagation in
673 shallow inlet/estuarine systems Part II: theory. Estuarine, Coastal and Shelf
674 Science 21, 207–224.

675 Temmerman S., Meire P., Bouma T.J., Herman P.M.J., Ysebaert T., de Vriend
676 H.J., 2013. Ecosystem-based coastal defense in the face of global change.
677 Nature 504, 79-83.

678 Townend I.H., Pethick J., 2002. Estuarine flooding and managed retreat.
679 Philosophical Transactions of the Royal Society A 360, 1477-1495.

680 Townend I.H., Whitehead P., 2003. A preliminary net sediment budget for the
681 Humber Estuary. Science of The Total Environment 314-316: 755-767.

682 Uehara K., Saito Y., Hori K., 2002. Paleotidal regime in the Changjiang
683 (Yangtze) estuary, the East China Sea, and the Yellow Sea at 6ka and 10 ka
684 estimated from a numerical model. Marine Geology 183, 79–192.

685 van der Wegen M., Roelvink J.A., 2008. Long-term morphodynamic evolution
686 of a tidal embayment using a two-dimensional, process-based model.
687 Journal of Geophysical Research 113, C03016, doi:10.1029/2006JC003983.

688 van Veen J., 1950. Ebb and flood-channel systems in The Netherlands tidal
689 water. Netherlands Geographical Studies 67, KNAG, Utrecht, pp.305–325. (in
690 Dutch)

691 Wang Z.H. Saito Y., Zhan Q., Nian X.M., Pan D.D., Wang L., Chen T., Xie J.L.,
692 Li X., Jiang X.Z., 2018. Three-dimensional evolution of the Yangtze River
693 mouth, China during the Holocene: impacts of sea level, climate and human
694 activity. Earth-Science Reviews 185, 938-955.

695 Wang Z.B., Elias E.P.L., van der Spek A.J.F., Lodder Q.J., 2018. Sediment
696 budget and morphological development of the Dutch Wadden Sea: impact of
697 accelerated sea-level rise and subsidence until 2100. Netherlands Journal of
698 Geosciences 97, 183-214.

699 Wu H., Zhu J.R., Chen B.R., Chen Y.Z., 2006. Quantitative relationship of
700 runoff and tide to saltwater spilling over from the North Branch in the
701 Changjiang Estuary: A numerical study. *Estuarine, Coastal and Shelf Science*
702 69, 125–132.

703 Yang H.F., Li B.C., Zhang C.Y., Qiao H.J., Liu Y.T., Bi J.F., Zhang Z.L., Zhou
704 F.N., 2020. Recent spatial-temporal variations of suspended sediment
705 concentrations in the Yangtze Estuary. *Water* 12, 818,
706 doi:10.3390/w12030818.

707 Yang O., Liu C.Z., 2002. Analysis on sediment transport patterns and sediment
708 sources of North Branch of Changjiang Estuary. *Journal of Hydraulic*
709 *Engineering* 2, 79-84. (in Chinese with an abstract in English)

710 Yu W.C., Lu J.Y., 2005. Morphological evolution and regulation of the
711 Changjiang River. China Water & Power Press, Beijing, 505 pp.

712 Yun C.X., 2004. Recent evolution of the Yangtze River estuary and its
713 mechanisms. China Ocean Press, Beijing, 302 pp. (in Chinese)

714 Yun C.X., 2010. A picture guide of the Yangtze River estuary evolution. China
715 Ocean Press, Beijing, 260 pp. (in Chinese)

716 Zhang C.Q., Cao H., 1998. Evolution trend of the North Branch in the
717 Changjiang Estuary. *Yangtze River* 29, 32-34.

718 Zhang E.F., Gao S., Savenije H.H.G., Si C.Y., Cao S., 2019. Saline water
719 intrusion in relation to strong winds during winter cold outbreaks: North
720 Branch of the Yangtze Estuary. *Journal of Hydrology* 574, 1099-1109.

721 Zhang J.H., Meng Y., 2009. Formation and evolution of the North Branch in the
722 Changjiang Estuary. *Yangtze River* 40(7), 14-17. (in Chinese)

723 Zhang J.Y., Huang Z.L., Hu Z.Y., 2007. Effect of reclamation project on the
724 North Branch of Yangtze River Estuary. *The Ocean Engineering* 25(2), 72-77.
725 (in Chinese with an abstract in English)

726 Zhang W., Feng H.C., Zhu Y.L., Zheng J.H., Hoitink A.J.F., 2020. Subtidal flow
727 reversal associated with sediment accretion in a delta channel. *Water*
728 *Resources Research* 55, <https://doi.org/10.1029/2019WR025945>.

729 Zou D.S., 1981. Hydro-morphodynamic changes in the recent 100 years and
730 the future trend of the North Branch in the Changjiang Estuary. *Jiangsu*
731 *Water Resources* 1, 52-64. (in Chinese)
732 Zou D.S., 1987. Morphological evolution and future trend of the North Branch
733 in the Changjiang Estuary. *Journal of Sediment Research* 1, 66-76.
734



737

738 **Figure S1.** Development of the Changjiang Delta and the North Branch
 739 illustrated in historical maps: (a) 1670, (b) 1705, (c) 1751, (d) 1824, (e) 1840, (f)
 740 1872, (g) 1900, (h) 1909, and (i) 1917. The big island in the river mouth is the
 741 Chongming Island, with the North Branch (NB) to the north of it. The space
 742 scales of the historical maps were not consistent and the maps are included
 743 here to display the topography changes but not for reference of detailed
 744 morphology.



745

746

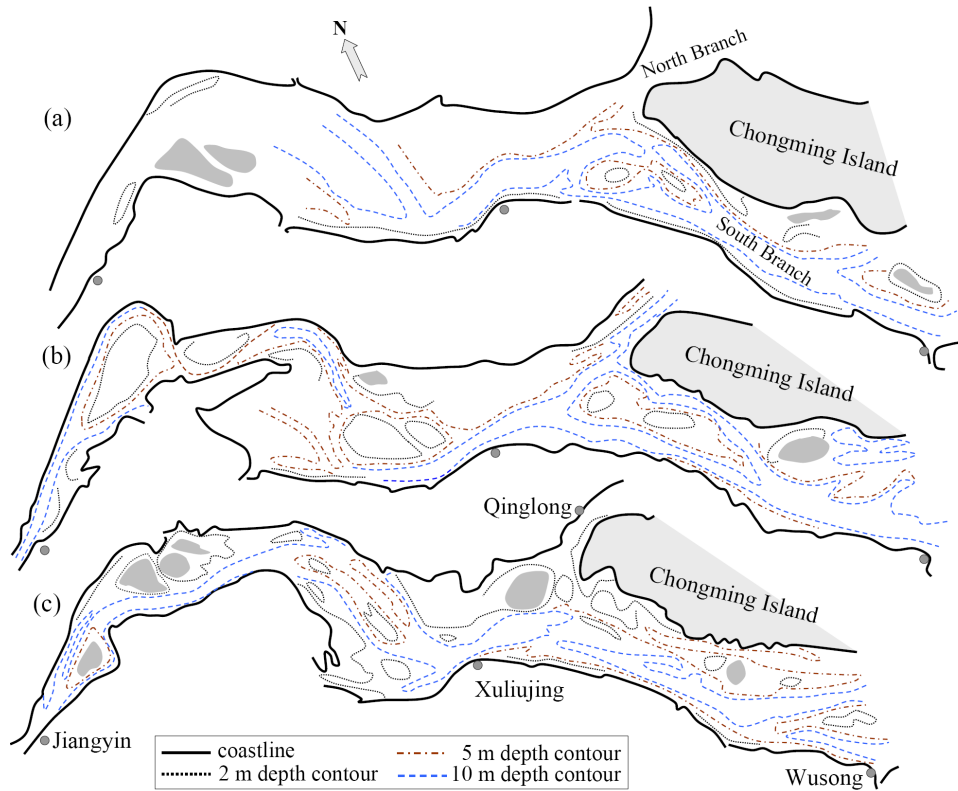
Figure S2. Illustrated topography changes of the North Branch in historical

747

maps in (a) 1915, (b) 1920, (c) 1927, and (d) 1940s. These maps are from

748

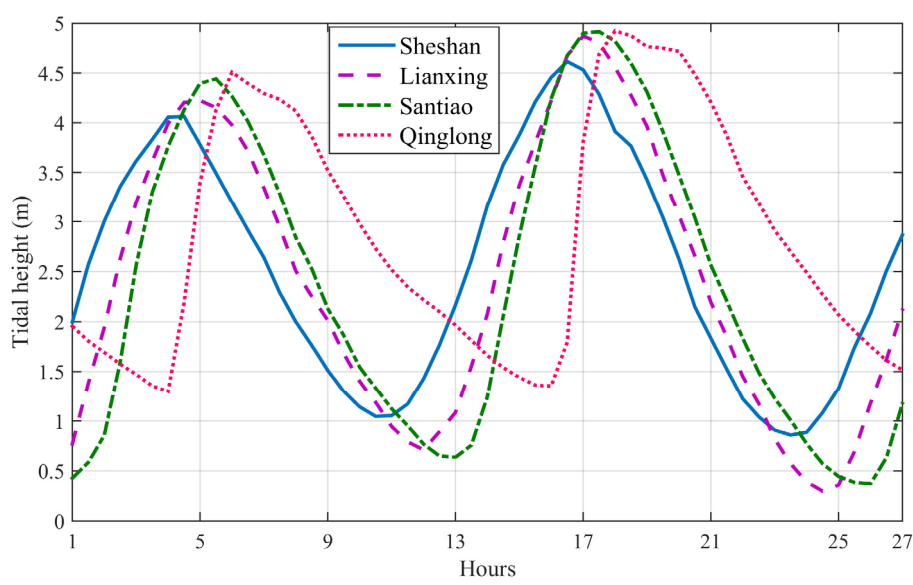
Virtual Shanghai website.



749

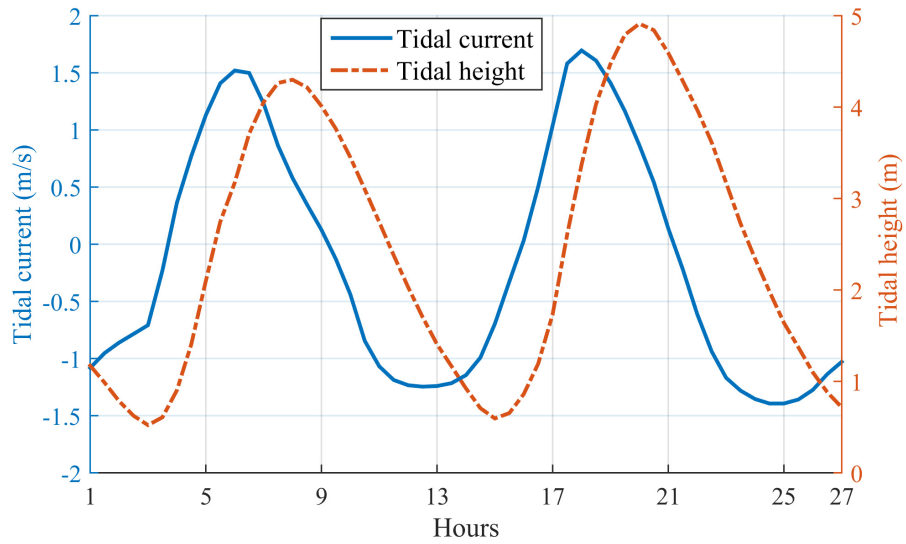
750 **Figure S3.** Sketches of the topography and depth contours of the
 751 Jianguyin-Wusong reaches and inflow section of the North Branch in (a) 1860,
 752 (b) 1915, and (c) 1958. Adopted from Yu and Lu (2005) and Yun (2004).

753



754

755 **Figure S4.** Tidal wave amplification and deformation inside the North Branch.
 756 Data were obtained in 1982.



757

758 **Figure S5.** Tidal currents and water level at a station close to Lianxing, which

759 shows stronger flood currents than ebb currents. Date measured in Nov. 2003

760 and adopted from Meng and Cheng (2005).